Fiber-Optical Analog of the Event Horizon

Thomas G. Philbin, *et al.*

Science **319**, 1367 (2008);
DOI: 10.1126/science.1153625

with the strength of the rule of law and also with cooperation levels suggests that the quality of the formal law enforcement institutions and informal sanctions are complements (rather than substitutes). Informal sanctions might be more effective in sustaining voluntary cooperation when the formal law enforcement institutions operate more effectively because antisocial punishment is lower in these societies. The detrimental effects of antisocial punishment on cooperation (and efficiency) also provide a further rationale why modern societies shun revenge and centralize punishment in the hands of the state.

References and Notes

1. E. Fehr, S. Gächter, *Nature* **415**, 137 (2002).
2. D. J. F. de Quervain *et al.*, *Science* **305**, 1254 (2004).
3. Ö. Gürerk, B. Irlenbusch, B. Rockenbach, *Science* **312**, 108 (2006).
4. B. Rockenbach, M. Milinski, *Nature* **444**, 718 (2006).
5. R. Axelrod, W. Hamilton, *Science* **211**, 1390 (1981).
6. M. A. Nowak, K. Sigmund, *Nature* **437**, 1291 (2005).
7. E. Ostrom, J. M. Walker, R. Gardner, *Am. Polit. Sci. Rev.* **86**, 404 (1992).
8. N. Nikiforakis, *J. Public Econ.* **92**, 91 (2008).
9. M. Cinyabuguma, T. Page, L. Putterman, *Exp. Econ.* **9**, 265 (2006).
10. L. Denant-Boemont, D. Masclet, C. N. Noussair, *Econ. Theory* **33**, 145 (2007).
11. J. Henrich *et al.*, *Behav. Brain Sci.* **28**, 795 (2005).
12. J. Henrich *et al.*, *Science* **312**, 1767 (2006).
13. Materials and methods are available on *Science* Online.
14. S. Knack, P. Keefer, *Q. J. Econ.* **112**, 1251 (1997).
15. G. Hofstede, *Culture's Consequences: Comparing Values, Behaviors, Institutions, and Organizations Across Nations* (Sage, Thousand Oaks, CA, 2001).
16. R. Inglehart, W. E. Baker, *Am. Sociol. Rev.* **65**, 19 (2000).
17. U. Fischbacher, *Exp. Econ.* **10**, 171 (2007).
18. A. Falk, E. Fehr, U. Fischbacher, *Econometrica* **73**, 2017 (2005).
19. J. Elster, *Ethics* **100**, 862 (1990).
20. D. Masclet, C. Noussair, S. Tucker, M. C. Villeval, *Am. Econ. Rev.* **93**, 366 (2003).
21. E. Fehr, S. Gächter, *Am. Econ. Rev.* **90**, 980 (2000).
22. T. Page, L. Putterman, B. Unel, *Econ. J.* **115**, 1032 (2005).
23. J. Coleman, *Foundations of Social Theory* (Belknap, Cambridge, MA, 1990).
24. J. Henrich, N. Henrich, *Why Humans Cooperate: A Cultural and Evolutionary Explanation*, Evolution and Cognition Series (Oxford Univ. Press, Oxford, 2007).
25. D. Kaufmann, A. Kraay, M. Mastruzzi, World Bank Policy Research Working Paper No. 4280, http://papers.ssrn.com/sol3/papers.cfm?abstract_id=999979
26. R. Boyd, P. J. Richerson, *Culture and the Evolutionary Process* (Univ. of Chicago Press, Chicago, 1985).
27. E. Ostrom, *Governing the Commons: The Evolution of Institutions for Collective Action, the Political Economy of Institutions and Decisions* (Cambridge Univ. Press, Cambridge, 1990).
28. R. J. Sampson, S. W. Raudenbush, F. Earls, *Science* **277**, 918 (1997).
29. R. B. Edgerton, *Sick Societies: Challenging the Myth of Primitive Harmony* (Free Press, New York, 1992).
30. T. H. Clutton-Brock, G. A. Parker, *Nature* **373**, 209 (1995).
31. W. B. G. Liebrand, R. W. T. L. Jansen, V. M. Rijken, C. J. M. Suhre, *J. Exp. Soc. Psychol.* **22**, 203 (1986).
32. K. Fliessbach *et al.*, *Science* **318**, 1305 (2007).
33. B. Monin, *Int. Rev. Soc. Psychol.* **20**, 53 (2007).
34. D. L. Bahry, R. K. Wilson, *J. Econ. Behav. Organ.* **60**, 37 (2006).
35. H. Hennig-Schmidt, Z.-Y. Li, C. Yang, *J. Econ. Behav. Organ.* **65**, 373 (2008).
36. J. Henrich, *J. Econ. Behav. Organ.* **53**, 3 (2004).
37. H. Bernhard, U. Fischbacher, E. Fehr, *Nature* **442**, 912 (2006).
38. J.-K. Choi, S. Bowles, *Science* **318**, 636 (2007).
39. H. C. Triandis, *Individualism and Collectivism*, R. E. Nisbett, Ed., *New Directions in Social Psychology* (Westview, Boulder, CO, 1995).
40. A. Dixit, *Lawlessness and Economics: Alternative Modes of Economic Governance* (Princeton Univ. Press, Princeton, NJ, 2004).
41. E. A. Posner, *Law and Social Norms* (Harvard Univ. Press, Cambridge, MA, 2000).
42. R. C. Ellickson, *Order Without Law: How Neighbors Settle Disputes* (Harvard Univ. Press, Cambridge, MA, 1991).
43. Alternative estimation methods, like Probit and Poisson, yield very similar results, both in terms of signs and statistical significance.

44. All authors contributed equally to this work. The authors thank various workshop audiences, in particular the Arts and Humanities Research Council workshops Culture and the Mind in Sheffield, and I. Bohnet, R. Boyd, S. Burks, E. Fehr, U. Fischbacher, D. Gambetta, H. Gintis, G. Grimalda, J. Henrich, P. Richerson, B. Rockenbach, R. Sapolsky, and R. Zeckhauser for helpful discussions. We are grateful for financial support from the University of Nottingham, the Grundlagenforschungsfonds at the University of St. Gallen, the Latsis Foundation (Geneva), and the EU-TMR Research Network ENDEAR (FMRX-CT98-0238). This paper is part of the MacArthur Foundation Network on Economic Environments and the Evolution of Individual Preferences and Social Norms.

Supporting Online Material

www.sciencemag.org/cgi/content/full/319/5868/1362/DC1
Materials and Methods
SOM Text
Figs. S1 to S4
Tables S1 to S10
References and Notes

5 December 2007; accepted 28 January 2008
10.1126/science.1153808

REPORTS

Fiber-Optical Analog of the Event Horizon

Thomas G. Philbin,[1,2] Chris Kuklewicz,[1] Scott Robertson,[1] Stephen Hill,[1] Friedrich König,[1] Ulf Leonhardt[1]*

The physics at the event horizon resembles the behavior of waves in moving media. Horizons are formed where the local speed of the medium exceeds the wave velocity. We used ultrashort pulses in microstructured optical fibers to demonstrate the formation of an artificial event horizon in optics. We observed a classical optical effect: the blue-shifting of light at a white-hole horizon. We also showed by theoretical calculations that such a system is capable of probing the quantum effects of horizons, in particular Hawking radiation.

Laboratory analogs of black holes (*1*–*3*) are inspired by a simple and intuitive idea (*4*): The space-time geometry of a black hole resembles a river (*5*, *6*)—a moving medium flowing toward a waterfall, the singularity. Imagine that the river carries waves propagating against the current with speed c'. The waves play the role of light, where c' represents c, the speed of light in vacuum. Suppose that the closer the river gets to the waterfall, the faster it flows, and that at some point the speed of the river exceeds c'. Clearly, beyond this point waves can no longer propagate upstream. The point of no return corresponds to the horizon of the black hole. Imagine another situation: a fast river flowing out into the sea, getting slower. Waves cannot enter the river beyond the point where the flow speed exceeds the wave velocity; the river resembles an object that nothing can enter: a white hole.

Nothing, not even light, can escape from a gravitational black hole. Yet according to quantum physics, the black hole is not entirely black but emits waves that are in thermal equilibrium (*7*–*9*). The waves consist of correlated pairs of quanta; one originates from inside and the other from outside the horizon. Seen from one side of the horizon, the gravitational black hole acts as a thermal black-body radiator sending out Hawking radiation (*7*–*9*). The effective temperature depends on the surface gravity (*7*–*9*), which, in the analog model, corresponds to the flow-velocity gradient at the horizon (*1*–*5*).

The Hawking temperature of typical black holes lies far below the temperature of the cosmic microwave background, so an observation of Hawking radiation in astrophysics seems unlikely. However, laboratory demonstrations of analogs of Hawking radiation could be feasible. One type of recent proposal (*10*–*12*) suggests the use of ultracold quantum gases such as alkali Bose-Einstein condensates or ultracold alkali fermions (*12*). When a condensate in a wave guide is pushed over a potential barrier, it may exceed the speed of sound (typically a few millimeters per second)

[1]School of Physics and Astronomy, University of St Andrews, North Haugh, St Andrews, Fife, KY16 9SS, UK. [2]Max Planck Research Group of Optics, Information and Photonics, Günther-Scharowsky-Strasse 1, Bau 24, D-91058 Erlangen, Germany.

*To whom correspondence should be addressed. E-mail: ulf@st-andrews.ac.uk

and is calculated to generate a Hawking temperature of about 10 nK (*11*). ^{3}H offers a multitude of analogs between quantum fluids and the standard model, including Einsteinian gravity (*2*). For example, the analogy between gravity and surface waves in fluids (*13*) has inspired ideas for artificial event horizons at the interface between two sliding superfluid phases (*14*), but so far, none of the quantum features of horizons has been measured in ^{3}H. Proposals for optical black holes (*15*, *16*) have relied on slowing down light (*17*) so that it matches the speed of the medium (*15*) or on bringing light to a complete standstill (*16*), but in these cases absorption may pose a severe problem near the horizon, where the spectral transparency window (*17*) vanishes.

On the other hand, is it necessary to physically move a medium to establish a horizon? What really matters are only the effective properties of the medium. If they change, for example as a propagating front, but the medium itself remains at rest, the situation is essentially indistinguishable from that in a moving medium. Such ideas have been discussed for moving solitons and domain walls (*18*) in superfluid ^{3}H (*2*) and more recently for microwave transmission lines with variable capacity (*19*), but they have remained impractical so far.

Here we report the first experimental observation of the classical optical effects of horizons, the blue-shifting of light at a white-hole horizon, and show theoretically that our scheme combines several promising features for demonstrating quantum Hawking radiation in the optical domain. Our idea, illustrated in Fig. 1, is based on the nonlinear optics of ultrashort light pulses in optical fibers (*20*), where we exploit the remarkable control of nonlinearity, birefringence, and dispersion that is possible in microstructured fibers (*21*, *22*).

Using a Ti:sapphire laser, we created 70-fs-long nondispersive pulses (solitons) at a carrier wavelength of 803 nm and a repetition rate of 80 MHz inside 1.5 m of microstructured fiber (NL-PM-750B from Crystal Fiber, Birkerød, Denmark). Each pulse modifies the optical properties of the fiber because of the Kerr effect (*20*): The effective refractive index of the fiber, n_0, gains an additional contribution δn that is proportional to the instantaneous pulse intensity I at position z and time t

$$n = n_0 + \delta n, \quad \delta n \propto I(z,t) \qquad (1)$$

This contribution to the refractive index n moves with the pulse. The pulse thus establishes a moving medium, although nothing material is moving. This effective medium naturally moves at the speed of light in the fiber, because it is made by light itself.

We also launched a continuous wave of light, a probe, that follows the pulse with slightly higher group velocity, attempting to overtake it. In order to distinguish the probe from the pulse, it oscillates at a significantly different frequency ω. Our probe-light laser is tunable over wavelengths $2\pi c/\omega$ from 1460 to 1540 nm. While approaching the pulse, the Kerr contribution δn slows down the probe until the probe's group velocity reaches the speed of the pulse. The trailing end of the pulse establishes a white-hole horizon, an object that light cannot enter, unless it tunnels through the pulse. Conversely, the front end creates a black-hole horizon for probe light that is slower than the pulse. Because δn is small, the initial group velocity of the probe should be sufficiently close to the speed of the pulse. In microstructured fibers (*22*), the group-velocity dispersion of light is engineered by arrangements of air holes (submicrometer-wide hollow cylinders along the fiber). We selected a fiber in which the group velocity of pulses near the 800-nm carrier wavelength of mode-locked Ti:sapphire lasers matched the group velocities of probes in the infrared telecommunication band around 1500 nm; standard optical fibers (*20*) do not have this property.

At the horizon of an astrophysical black hole, light freezes, reaching wavelengths shorter than the Planck scale, where the physics is unknown. [The Planck length is given by $\sqrt{\{hG/c^3\}}$, where G is the gravitational constant.] Some elusive trans-Planckian mechanism must regularize this behavior (*23*, *24*). In our case, the fiber-optical analog of trans-Planckian physics is known and simple—it is contained in the frequency dependance of the refractive index n, the dispersion of the fiber. At the trailing end of the pulse, the incoming probe modes are compressed, oscillating with increasing frequency; they are blue-shifted. In turn, the dispersion limits the frequency shifting by tuning the probe out of the horizon. In the case of normal group-velocity dispersion, the blue-shifted light falls behind. At the black-hole horizon, the reverse occurs: A probe slower than the pulse is red-shifted and then moves ahead of the pulse.

Figure 2 shows the difference in the spectrum of the probe light (incident with ω_1) with and without the pulses, clearly displaying a blue-shifted peak at ω_2. To quantitatively describe this effect, we consider the frequency ω' in a co-moving frame that is connected to the laboratory frame frequency ω by the Doppler formula

$$\omega' = \left(1 - \frac{nu}{c}\right)\omega \qquad (2)$$

For a stable pulse, ω' is a conserved quantity, whereas ω follows the contours of fixed ω' when δn varies with the intensity profile of the pulse (Fig. 3). For sufficiently large δn, the frequency ω completes an arch from the initial ω_1 to the final ω_2; it is blue-shifted by the white-hole horizon. At a black-hole horizon, the arch is traced the other way round from ω_2 to ω_1. For the frequency at the center of the arches, an infinitesimal δn is sufficient to cause a frequency shift; at this frequency, the group velocity of the probe matches the group velocity of the pulse. Figure 2 shows that both the blue-shifted and probe light are spectrally broadened. These features are easily explained: The horizon acts only during the time while probe and pulse propagate in the fiber, where only a finite fraction of the probe is frequency-shifted, forming a blue-shifted pulse and also a gap in the probe light, a negative pulse; these pulses have a characteristic spectrum with a width that is inversely proportional to the fiber length. We compared the measured spectra with the theory of light propagation in the presence of horizons and found very good agreement (*25*).

Imagine instead of a single probe a set of probe modes. The modes should be sufficiently weakly excited that they do not interact with each other via the Kerr effect, but they experience the cross Kerr effect of the pulse, the presence of the medium (Eq. 1) moving with the velocity u. The modes constitute a quantum field of light in a moving medium (*25*, *26*). Classical light is a real electro-

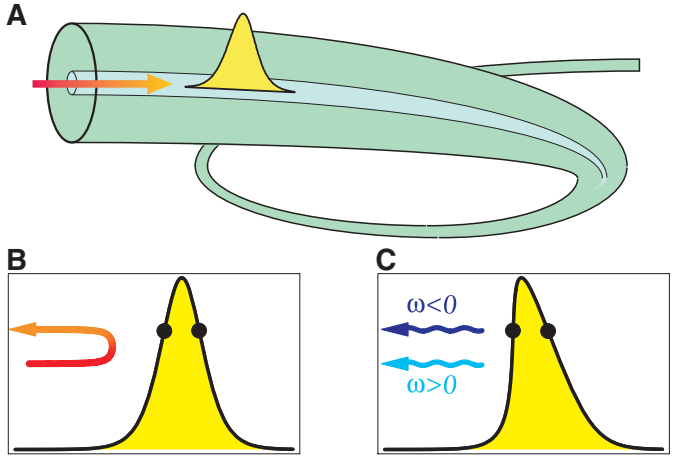

Fig. 1. Fiber-optical horizons. (**A**) A light pulse in a fiber slows down infrared probe light, attempting to overtake it. The diagrams below are in the co-moving frame of the pulse. (**B**) Classical horizons. The probe is slowed down by the pulse until its group velocity matches the pulse speed at the points indicated by black dots, establishing a white-hole horizon at the back and a black-hole horizon at the front of the pulse. The probe light is blue-shifted at the white hole until the optical dispersion releases it from the horizon. (**C**) Quantum pairs. Even if no probe light is incident, the horizon emits photon pairs corresponding to waves of positive frequencies from the outside of the horizon paired with waves at negative frequencies from beyond the horizon. An optical shock has steepened the pulse edge, increasing the luminosity of the white hole.

magnetic wave. So, according to Fourier analysis, any amplitude oscillating as $\exp(-i\omega\tau)$ at a positive angular frequency ω must be accompanied by the complex conjugate amplitude at $-\omega$. In quantum field theory (*8*, *9*, *25*), the positive-frequency modes correspond to the annihilation operators and the negative-frequency modes to the creation operators (*26*). Processes that mix positive and negative frequencies in the laboratory frame (in the glass of the fiber) thus create observable light quanta.

In the near ultraviolet around 300 nm, the dispersion of microstructured fibers (*22*) is dominated by the bare dispersion of glass, where n_0 rapidly grows with frequency (*20*) exceeding c/u. For such ultraviolet modes, the medium moves at superluminal speed. We see from the Doppler formula (Eq. 2) that these superluminal modes oscillate with negative frequencies ω' in the co-moving frame for positive frequencies ω in the laboratory frame, and vice versa. Moreover, each subluminal mode with positive ω has a superluminal partner oscillating at the same co-moving frequency ω' but with negative laboratory frequency. The pulse does not change ω', but it may partially convert sub- and superluminal partner modes into each other, thus creating photons (*8*, *9*). Even if all the modes are initially in their vacuum states, the horizon spontaneously creates photon pairs. This process represents the optical analog of Hawking radiation (*7*), and it occurs at both the black-hole and white-hole horizon (*25*). Photons with positive ω' correspond to the particles created at the outside of the black hole (*8*, *9*), whereas the negative-frequency photons represent their partners beyond the horizon. In our case, the photon pairs are distinguishable from the intense pulse, because their polarization can be orthogonal to the pulse and their frequencies differ from the carrier frequency by an octave. Furthermore, one can discriminate the Hawking effect from other nonlinear optical processes, such as four-wave mixing, because it is not subject to their phase-matching conditions (*20*). Moreover, in addition to observing Hawking radiation per se, one could detect the correlations of the Hawking partners—a feat that is impossible in astrophysics, because there the partner particles are lost beyond the horizon of the black hole.

In order to give a quantitative argument for the Hawking effect in optical fibers, we describe the propagation distance z in terms of the time ζ it takes for the pulse to traverse it, $\zeta = z/u$, and introduce the retarded time $\tau = t - z/u$. The phase φ of each mode evolves as

$$\varphi = -\int(\omega d\tau + \omega' d\zeta) \tag{3}$$

We assume that the mode conversion occurs in a narrow interval of retarded time τ near a horizon around $\tau = 0$, where we linearize δn in τ such that

$$1 - \frac{nu}{c} = \alpha'\tau \tag{4}$$

We obtain from the phase integral (Eq. 3) and the Doppler formula (Eq. 2) the characteristic logarithmic phase at a horizon (*8*, *9*). We use the standard result (*8*, *9*, *25*): Hawking radiation is Planck-distributed with the temperature

$$k_B T' = \frac{\hbar\alpha'}{2\pi} \tag{5}$$

where k_B denotes Boltzmann's constant. For evaluating α', we consider δn at $\tau = 0$, where

$$\alpha' = -\frac{u}{c}\frac{\partial n}{\partial \tau}\bigg|_0 = -\frac{u}{c}\frac{\partial \delta n}{\partial \tau}\bigg|_0 \tag{6}$$

Note that T' denotes the Hawking temperature in the co-moving frame, defined with respect to the Doppler-shifted frequencies ω', a temperature that is characterized by the Doppler-shifted Hawking frequency α' in regions away from the pulse. We use the Doppler formula (Eq. 2) with the refractive index (Eq. 1) and the linearization (Eq. 4) taken at $\tau = 0$, and obtain

$$\alpha' = \left(1 - n_0\frac{u}{c}\right)\alpha = \frac{u}{c}\delta n\Big|_0\,\alpha \tag{7}$$

Consequently, the Hawking temperature T in the laboratory frame is

$$k_B T = \frac{\hbar\alpha}{2\pi}, \quad \alpha = -\frac{1}{\delta n}\frac{\partial \delta n}{\partial \tau}\bigg|_0 \tag{8}$$

Because T does not depend on the magnitude of δn, even the typically very small refractive index variations of nonlinear fiber optics (*20*) may lead to a substantial Hawking temperature when δn varies on the scale of an optical wavelength. This is achievable with optical pulses of a few cycles (*27*, *28*).

The Kerr nonlinearity (*20*) influences not only the probe modes but the pulse as well (*20*). This self–Kerr effect shapes the pulse while it propagates in the fiber. Regions of high intensity lag behind, because for them the effective refractive index is increased. The black-hole horizon at the front is stretched, but the trailing edge becomes extremely steep, infinitely steep in theory (*20*): The pulse develops an optical shock (*20*). The steep white-hole horizon will dominate the Hawking effect of the pulse. In practice, dispersion combined with other nonlinear optical

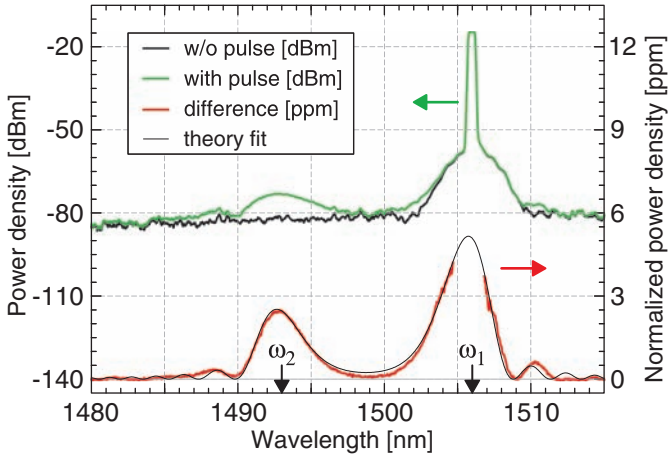

Fig. 2. Measurement of blue-shifting at a white-hole horizon. The black curve shows the power spectrum of probe light that has not interacted with the pulses, whereas the green curve displays the result of the interaction; both curves are represented on a logarithmic scale. The difference between the spectra on a linear scale, shown in red, exhibits a characteristic peak around the blue-shifted wavelength (ω_2) and another peak around the spectral line of the probe laser (ω_1) due to a gap in the probe light; both features indicate the presence of a horizon. ppm, parts per million.

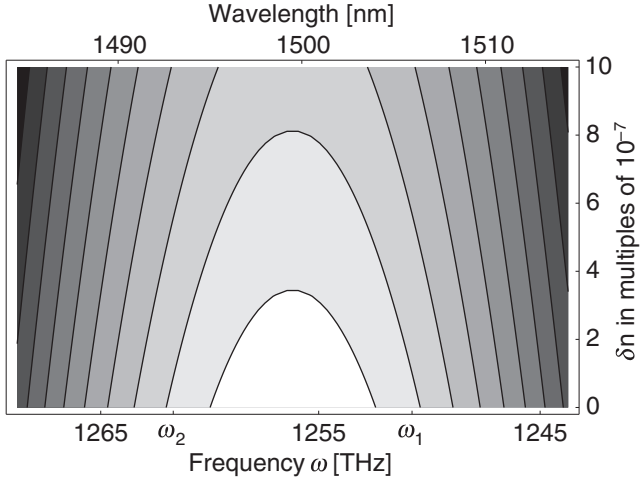

Fig. 3. Doppler contours. The Doppler-shifted frequency ω' of the probe is a conserved quantity. The pulse shifts the laboratory frequency ω along the contour lines of ω' as a function of the instantaneous δn; the same applies to the wavelength $\lambda = 2\pi c/\omega$. If the pulse is sufficiently intense that δn reaches the top of a contour, the probe light completes an arch on the diagram while leaving the pulse; it is red- or blue-shifted, depending on its initial frequency.

processes in the fiber, in particular stimulated Raman scattering (*20*), limit the optical shock. Assuming that the steepness at the shock front is comparable to twice the frequency of the pulse carrier, 8×10^{14} Hz, the Hawking temperature (Eq. 8) reaches 10^3 K, which is many orders of magnitude higher than that in condensed-matter analogs of the event horizon (*10*–*12*, *18*).

Our scheme thus solves two problems at once in a natural way: how to let an effective medium move at superluminal speed, and how to generate a steep velocity profile at the horizon. Here the various aspects of the physics of artificial black holes conspire together, in contrast to most other proposals (*1*–*4*, *10*–*16*).

References and Notes

1. *Artificial Black Holes*, M. Novello, M. Visser, G. E. Volovik, Eds. (World Scientific, Singapore, 2002).
2. G. E. Volovik, *The Universe in a Helium Droplet* (Clarendon Press, Oxford, 2003).
3. W. G. Unruh, R. Schützhold, *Quantum Analogues: From Phase Transitions to Black Holes and Cosmology* (Springer, Berlin, 2007).
4. W. G. Unruh, *Phys. Rev. Lett.* **46**, 1351 (1981).
5. T. Jacobson, *Prog. Theor. Phys.* **136** (suppl.), 1 (1999).
6. G. Rousseaux, C. Mathis, P. Maïssa, T. G. Philbin, U. Leonhardt, http://arxiv.org/abs/0711.4767.
7. S. M. Hawking, *Nature* **248**, 30 (1974).
8. N. D. Birrell, P. C. W. Davies, *Quantum Fields in Curved Space* (Cambridge Univ. Press, Cambridge, 1984).
9. R. Brout, S. Massar, R. Parentani, Ph. Spindel, *Phys. Rep.* **260**, 329 (1995).
10. L. J. Garay, J. R. Anglin, J. I. Cirac, P. Zoller, *Phys. Rev. Lett.* **85**, 4643 (2000).
11. S. Giovanazzi, C. Farrell, T. Kiss, U. Leonhardt, *Phys. Rev. A* **70**, 063602 (2004).
12. S. Giovanazzi, *Phys. Rev. Lett.* **94**, 061302 (2005).
13. R. Schützhold, W. G. Unruh, *Phys. Rev. D* **66**, 044019 (2002).
14. G. E. Volovik, *J. Exp. Theor. Phys. Lett.* **76**, 240 (2002).
15. U. Leonhardt, P. Piwnicki, *Phys. Rev. Lett.* **84**, 822 (2000).
16. U. Leonhardt, *Nature* **415**, 406 (2002).
17. P. W. Milonni, *Fast Light, Slow Light and Left Handed Light* (Institute of Physics, Bristol, UK, 2004).
18. T. A. Jacobson, G. E. Volovik, *Phys. Rev. D* **58**, 064021 (1998).
19. R. Schützhold, W. G. Unruh, *Phys. Rev. Lett.* **95**, 031301 (2005).
20. G. Agrawal, *Nonlinear Fiber Optics* (Academic Press, San Diego, CA, 2001).
21. W. H. Reeves *et al.*, *Nature* **424**, 511 (2003).
22. P. Russell, *Science* **299**, 358 (2003).
23. G. t'Hooft. *Nucl. Phys. B* **256**, 727 (1985).
24. T. Jacobson, *Phys. Rev. D* **44**, 1731 (1991).
25. See the supporting material on *Science* Online.
26. U. Leonhardt, *Rep. Prog. Phys.* **66**, 1207 (2003).
27. *Few-Cycle Laser Pulse Generation and Its Applications*, F. X. Kärtner, Ed. (Springer, Berlin, 2004).
28. T. Brabec, F. Krausz, *Rev. Mod. Phys.* **72**, 545 (2000).

29. We are indebted to G. Agrawal, M. Dunn, T. Hänsch, A. Miller, R. Parentani, and W. Sibbett for discussions and technical support. We thank A. Podlipensky and P. Russell for measuring the dispersion of our fiber. Our work was supported by the Leverhulme Trust, Engineering and Physical Sciences Research Council, Continuous Variable Quantum Information with Atoms and Light, the Ultrafast Photonics Facility at St Andrews, and Leonhardt Group Aue.

Supporting Online Material

www.sciencemag.org/cgi/content/full/319/5868/1367/DC1
SOM Text
Figs. S1 to S13
Table S1
References and Notes

30 November 2007; accepted 24 January 2008
10.1126/science.1153625

Stimuli-Responsive Polymer Nanocomposites Inspired by the Sea Cucumber Dermis

Jeffrey R. Capadona,[1,2,3] Kadhiravan Shanmuganathan,[1] Dustin J. Tyler,[2,3] Stuart J. Rowan,[1,2,3,4]* Christoph Weder[1,2,4]*

Sea cucumbers, like other echinoderms, have the ability to rapidly and reversibly alter the stiffness of their inner dermis. It has been proposed that the modulus of this tissue is controlled by regulating the interactions among collagen fibrils, which reinforce a low-modulus matrix. We report on a family of polymer nanocomposites, which mimic this architecture and display similar chemoresponsive mechanic adaptability. Materials based on a rubbery host polymer and rigid cellulose nanofibers exhibit a reversible reduction by a factor of 40 of the tensile modulus, for example, from 800 to 20 megapascals (MPa), upon exposure to a chemical regulator that mediates nanofiber interactions. Using a host polymer with a thermal transition in the regime of interest, we demonstrated even larger modulus changes (4200 to 1.6 MPa) upon exposure to emulated physiological conditions.

Many echinoderms share the ability to rapidly and reversibly alter the stiffness of their connective tissue (*1*). In the case of sea cucumbers (Fig. 1, A and B), this morphing occurs within seconds and creates considerable survival advantages (*1*, *2*). A series of recent studies on the dermis of these invertebrates has provided evidence that this defense mechanism is enabled by a nanocomposite structure in which rigid, high-aspect ratio collagen fibrils reinforce a viscoelastic matrix of fibrillin microfibrils (*2*–*4*). The stiffness of the tissue is regulated by controlling the stress transfer between adjacent collagen fibrils through transiently established interactions (*5*, *6*). These interactions are modulated by soluble macromolecules that are secreted locally by neurally controlled effector cells. The dermis of the *Cucumaria frondosa* and other sea cucumber species represents a compelling model of a chemoresponsive material in which a modulus contrast by a factor of 10 (~5 to ~50 MPa) is possible (*7*). Intrigued by this capability and with the goal of creating new dynamic materials for biomedical applications, we set out to investigate whether nanocomposites can be created that exhibit similar architecture and properties. The control of nanofiber interactions exploited here in solid polymer materials is similar to that observed in aqueous dispersions of poly(acrylic acid)-coated carbon nanotubes (*8*) or cellulose nanofibers (*9*), which have been shown to exhibit large viscosity changes upon variation of pH. The materials further complement other polymeric systems with morphing mechanical behavior—for example, cross-linked polymers that change cross-link density upon a change in pH or ionic concentration (*10*, *11*).

The first series of nanocomposites studied is based on a rubbery ethylene oxide–epichlorohydrin 1:1 copolymer (EO-EPI) (Fig. 1C) into which a rigid cellulose nanofiber network was incorporated (Fig. 1, C and D). The EO-EPI matrix displays a low modulus and can accommodate the uptake of several chemical stimuli. Cellulose nanofibers, isolated for this study from the mantles of sessile sea creatures known as tunicates (*12*), were used as the reinforcing component. These "whiskers" exhibit high stiffness (tensile modulus ~143 GPa) (*13*) and dimensions at the nanometer scale (26 nm × 2.2 μm) (fig. S1). Similar nanofibers can be obtained from a range of renewable biosources, including wood and cotton. Whiskers from tunicates were used here because their aspect ratio is higher than that of cellulose from other sources, which is advantageous for the formation of percolating architectures. Because of the high density of strongly interacting surface hydroxyl groups, cellulose whiskers have a strong tendency for aggregation (*9*, *14*). The whisker-whisker interactions can be moderated by the introduction of sulfate surface groups (Fig. 1C), which promote dispersibility in select hydrogen-bond–forming solvents (*14*, *15*). This balance of attractive and repulsive interactions is the key for the fabrication of cellulose-whisker nanocomposites.

[1]Department of Macromolecular Science and Engineering, Case Western Reserve University, Cleveland, OH 44106, USA. [2]Rehabilitation Research and Development, Louis Stokes Cleveland DVA Medical Center, 10701 East Boulevard, Cleveland, OH 44106, USA. [3]Department of Biomedical Engineering, Case Western Reserve University, Cleveland, OH 44106, USA. [4]Department of Chemistry, Case Western Reserve University, 10900 Euclid Avenue, Cleveland, OH 44106, USA.

*To whom correspondence should be addressed. E-mail: christoph.weder@case.edu (C.W.); stuart.rowan@case.edu (S.J.R.)